Water and Halide Adsorption to Corrosion Surfaces: Molecular Simulations of Atmospheric Interactions with Aluminum Oxyhydroxide and Gold

Louise J. Criscenti,* Randall T. Cygan, Ara S. Kooser, and Harold K. Moffat

Sandia National Laboratories, Albuquerque, New Mexico 87185-0754

Atmospheric corrosion due to adsorption of water and solutes onto metal and metal oxide surfaces is a critical factor in the long term reliability of electronic devices. To investigate the atomistic mechanisms of corrosion, we used molecular dynamics (MD) simulations to study the structure of water adsorbed onto both boehmite (γ-AlO(OH)) and gold (Au) surfaces and electrolyte adsorption and surface speciation on the boehmite (010) surface. Boehmite forms a thin film on aluminum metal under oxidizing conditions, is hydrophilic, and readily adsorbs water from the atmosphere. In contrast, gold surfaces are hydrophobic, and condensed water does not readily bond with the surface. Our MD simulations were performed using the CLAYFF force field that maintains full flexibility of water and substrate and allows for full energy and momentum transfer among all atoms. The boehmite (010) and gold (111) surfaces were initially simulated with no water present and then with incremental additions of water molecules. The calculations indicate the boehmite (010) surface structure strongly controls the organization of the first monolayer of interfacial water. In contrast, the structure of water on the gold (111) surface is controlled by hydrogen bonding among the water molecules. To investigate Cl^- adsorption to the boehmite surface, Na^+ and Cl^- ions were added to two boehmite−water simulation cells, one with 3.5 monolayers of water on the boehmite surface and the other representing water-saturated conditions. In both scenarios, the addition of NaCl solute disturbed the first monolayer of water adsorbed to the surface. Chloride ions displaced water molecules that were originally bound to the boehmite surface. In contrast, the Na^+ ions do not disturb the arrangement of these water molecules. Na^+−Cl^- pairs were observed to occur on the surface. Both the near-surface water structure and the effects of ion adsorption were similar regardless of the number of monolayers of water present in the simulation cells.

Background

Metals such as Al exhibit a significant degree of corrosion resistance in a wide variety of environments due to the presence of protective surface oxides. Boehmite, an Al-oxyhydroxide (γ-AlO(OH)), is one of the several aluminum oxides, oxyhydroxides, and hydroxides that form upon the oxidation of aluminum[1,2] and has been observed in the passive thin films protecting Al metal and Al-metal alloys.[3,4] Gold is representative of common connector and post materials used in microelectronics; it often coexists with Al components in circuits and related devices and does not react with the environment to form a protective oxide coating.

Exposure of Al metal to halides like chloride (Cl^-) results in pitting corrosion. In pitting, the metal corrosion is extremely localized and is typically initiated at a lattice defect site expressed on the metal surface. Pit initiation may involve the transport of aggressive anions such as Cl^- through the passive oxide/hydroxide film to the interface with Al metal

where aggressive dissolution is promoted. Or pit initiation may occur by a film-breaking mechanism in which Cl^- adsorption to the Al-hydroxide surface is the first step in passive film thinning. These theories are discussed in detail in many metal corrosion review papers[5–7] and are supported by spectroscopic observations that chloride is taken up by oxide thin films[8–13] prior to pit initiation.

First-principles and atomistic molecular dynamics simulations have been used in the past to establish the sites of water molecule dissociation or physisorption on oxides such as MgO,[14,15] CaO,[14] α-TiO$_2$,[16] α-SiO$_2$,[17–20] α-Al$_2$O$_3$,[21,22] and

---

* Corresponding author. E-mail: ljcrisc@sandia.gov.

(1) Lopez, S.; Petit, J.-P.; Dunlop, H. M.; Butruille, J.-R.; Tourillon, G. *J. Electrochem. Soc.* **1998,** *145,* 823.
(2) Lopez, S.; Petit, J.-P.; Tourillon, G.; Dunlop, H. M.; Butruille, J.-R. *J. Electrochem. Soc.* **1998,** *145,* 829.
(3) Ahmad, Z.; Aleem, B. J. A. *Mater. Des.* **2002,** *23,* 173.
(4) Rotole, J. A.; Sherwood, P. M. A. *Fresenius' J. Anal. Chem.* **2001,** *369,* 342.

(5) Strehblow, H. H. *Werkstoffe und Korrosion* **1984,** *35,* 437.
(6) Frankel, G. S. *J. Electrochem. Soc.* **1998,** *145,* 2186.
(7) Bohni, H. Localized Corrosion of Passive Metals. In *Uhlig's Corrosion Handbook*; Revie, W., Ed.; John Wiley & Sons, Inc.: New York, 2000; p 173.
(8) Natishan, P. M.; O'Grady, W. E.; McCafferty, E.; Ramaker, D. E.; Pandya, K.; Russell, A. *J. Electrochem. Soc.* **1999,** *146,* 1737.
(9) Yu, S. Y.; O'Grady, W. E.; Ramaker, D. E.; Natishan, P. M. *J. Electrochem. Soc.* **2000,** *147,* 2952.
(10) Natishan, P. M.; Yu, S. Y.; O'Grady, W. E.; Ramaker, D. E. *Electrochim. Acta* **2002,** *47,* 3131.
(11) Kolics, A.; Polkinghorne, J. C.; Wieckowski, A. *Electrochim. Acta* **1998,** *43,* 2605.
(12) Kolics, A.; Polkinghorne, J. C.; Thomas, A. E.; Wieckowski, A. *Chem. Mater.* **1998,** *10,* 812.
(13) Kolics, A.; Besing, A. S.; Baradlai, P.; Haasch, R.; Wieckowski, A. *J. Electrochem. Soc.* **2001,** *148,* B251.
(14) Carrasco, J.; Illas, F.; Lopez, N. *Phys. Rev. Lett.* **2008,** *100,* 016101.

α-Fe$_2$O$_3$.[23] These studies have contributed to our understanding of the formation of hydroxylated surface sites in an atmospheric environment. The adsorption of water to hydroxylated oxides (i.e., rutile (α-TiO$_2$),[24] cassiterite (SnO$_2$),[25] quartz (α-SiO$_2$)[18]), hydroxides (i.e., brucite (Mg(OH)$_2$),[26] gibbsite (Al(OH)$_3$),[26] white rust (Fe(OH)$_2$)[23]), and oxyhydroxides (i.e., goethite (α-FeO(OH))[23]) has also been simulated to investigate water structure at solid−water interfaces. Most molecular dynamics simulations of crystal−water interactions implement a point charge model for water. However, polarizable and dissociative water models have also been developed and used to investigate associative and dissociative adsorption of water to oxide surfaces.[15,17−20,23,27−35]

In this study, a series of classical molecular dynamics simulations was used to investigate the adsorption of water molecules and chloride on an Al-oxyhydroxide boehmite (γ-AlO(OH)), a representative passivating, thin film-forming oxyhydroxide on Al metal under atmospheric conditions. In addition, water adsorption to the gold (111) surface was simulated to qualitatively compare the calculated adsorption energies and water structure as a function of relative humidity on a hydrophilic surface (i.e., boehmite (010)) and a relatively hydrophobic surface (i.e., Au(111)).

Simulation Methods

Molecular dynamics simulations were performed using the CLAYFF force field originally developed to study hydroxide and aluminosilicate mineral−water interactions.[36] This force field is based on an ionic (nonbonded) description of the metal−oxygen interactions within hydrated crystalline compounds. CLAYFF incorporates the simple point charge (SPC) water model[37] to represent the bonded and nonbonded interactions for water molecules and surface hydroxyl groups. Bond stretch and bond angle terms are introduced into the standard SPC water model to provide full flexibility for the water molecules and hydroxyl groups.[38] The total energy, E_{total}, calculated with CLAYFF, has contributions from Coulombic (electrostatic), short-range (van der Waals), and bonded interactions:

$$E_{total} = E_{coul} + E_{VDW} + E_{bondstretch} + E_{anglebend} \qquad (1)$$

The interactions within boehmite are described primarily by the Coulombic and van der Waals energy terms. The bond stretch and angle bend energy terms are represented by harmonic functions in the flexible SPC water model used to describe adsorbing water molecules and hydroxyl groups both within the bulk and on the surface of the boehmite. The full atomic flexibility of CLAYFF allows the exchange of momentum and energy across all atoms, in the crystal structure, the aqueous phase, and the interface. CLAYFF has already been shown to successfully simulate the interaction of other hydroxide surfaces with aqueous solutions.[39−41] To investigate the adsorption of Na$^+$ and Cl$^-$ onto boehmite, accurate force field parameters for aqueous Na$^+$ and Cl$^-$ ions[42] were incorporated into CLAYFF.

For comparison with boehmite, we also performed molecular simulations of water adsorption onto a gold surface. The Lennard-Jones parameters for gold were taken from the charge valence force field[43] (CVFF) and incorporated into the CLAYFF parameter set. Conventional combination rules were applied to generate the nonbonded parameters between specific atom pairs.[44] No partial charges were assigned to the gold atoms; all water and electrolyte interactions with the gold surface are represented solely by the van der Waals interactions. All molecular dynamics simulations were performed using the Cerius^2 (Accelrys, Inc.[45]) open force field (OFF) module, using a spline function with cutoffs of 8.0 Å and 8.5 Å (to ensure a smooth transition to zero energy) to calculate the van der Waals energies and a Ewald summation with a real space cut off of 10.85 Å (and $\eta = 3.21$) to evaluate the long-range Coulombic interactions.

Boehmite (010) and Gold (111) Surfaces. The boehmite (010) surface model was created based on published unit

(15) de Leeuw, N. H.; Parker, S. C. *Phys. Rev. B* **1998**, *58*, 13901.
(16) Bandura, A. V.; Sykes, D. G.; Shapovalov, V.; Truong, T. N.; Kubicki, J. D.; Evarestov, R. A. *J. Phys. Chem. B* **2004**, *108*, 7844.
(17) de Leeuw, N. H.; Higgins, F. M.; Parker, S. C. *J. Phys. Chem. B* **1999**, *103*, 1270.
(18) Du, Z.; de Leeuw, N. H. *Dalton Trans.* **2006**, 2623.
(19) Garofalini, S. H. *J. Non-Cryst. Solids* **1990**, *120*, 1.
(20) Mahadevan, T. S.; Garofalini, S. H. *J. Phys. Chem. B* **2007**, *111*, 8919.
(21) Hass, K. C.; Schnieder, W. F.; Curioni, A.; Andreoni, W. *J. Phys. Chem. B* **2000**, *104*, 5527.
(22) de Leeuw, N. H.; Parker, S. C. *J. Am. Ceram. Soc.* **1999**, *82*, 3209.
(23) de Leeuw, N. H.; Cooper, T. G. *Geochim. Cosmochim. Acta* **2007**, *71*, 1655.
(24) Predota, M.; Bandura, A. V.; Cummings, P. T.; Kubicki, J. D.; Wesolowski, D. J.; Chialvo, A. A.; Machesky, M. L. *J. Phys. Chem. B* **2004**, *108*, 12049.
(25) Vlcek, L.; Zhang, Z.; Machesky, M. L.; Fenter, P. A.; Rosenqvist, J.; Wesolowski, D. J.; Anovitz, L. M.; Predota, M.; Cummings, P. T. *Langmuir* **2007**, *23*, 4925.
(26) Wang, J.; Kalinichev, A. G.; Kirkpatrick, R. J. *Geochim. Cosmochim. Acta* **2006**, *70*, 562.
(27) Rustad, J. R.; Felmy, A. R.; Hay, B. P. *Geochim. Cosmochim. Acta* **1996**, *60*, 1553.
(28) Rustad, J. R.; Felmy, A. R.; Hay, B. P. *Geochim. Cosmochim. Acta* **1996**, *60*, 1563.
(29) de Leeuw, N. H.; Parker, S. C. *J. Am. Ceram. Soc.* **1999**, *82*, 3209.
(30) Rustad, J. R.; Wasserman, E.; Felmy, A. R.; Wilke, C. *J. Colloid Interface Sci.* **1998**, *198*, 119.
(31) Rustad, J. R.; Wasserman, E.; Felmy, A. R. *Surf. Sci.* **1999**, *424*, 28.
(32) Wasserman, E.; Rustad, J. R.; Felmy, A. R. *Surf. Sci.* **1999**, *424*, 17.
(33) Rustad, J. R.; Felmy, A. R. Molecular statics calculations of acid/base reactions on magnetite (001). In *Solid-Liquid Interface Theory*; Halley, J. W., Ed.; ACS Symposium Series 789; American Chemical Society: Washington, DC, 2001; Chapter 9, p 113.
(34) Rustad, J. R.; Wasserman, E.; Felmy, A. R. The magnetite (001) surface: Insights from molecular dynamics calculations. In *Properties of Complex Inorganic Solids*; Meike, A., Gonis, A., Turchi, P. E. A., Rajan, K., Eds.; Kluwer Academic/Plenum Publishers: Dordrecht, 2000; Vol. II; p 499.
(35) Rustad, J. R.; Felmy, A. R.; Bylaska, E. J. *Geochim. Cosmochim. Acta* **2003**, *67*, 1001.
(36) Cygan, R. T.; Liang, J.-J.; Kalinichev, A. G. *J. Phys. Chem. B* **2004**, *108*, 1255.
(37) Berendsen, H. J. C.; Postma, J. P. M.; van Gunsteren, W. F.; Hermans, J. Interaction models for water in relation to protein hydration. In *Intermolecular Forces*; Pullman, B., Ed.; D. Reidel: Dordrecht, 1981; p 331.
(38) Teleman, O.; Jonsson, B.; Engstrom, S. *Mol. Phys.* **1987**, *60*, 193.
(39) Wang, J.; Kalinichev, A. G.; Kirkpatrick, R. J.; Hou, X. *Chem. Mater.* **2001**, *13*, 145.
(40) Kalinichev, A. G.; Kirkpatrick, R. J. *Chem. Mater.* **2002**, *14*, 3539.
(41) Hou, X.; Kalinichev, A. G.; Kirkpatrick, R. J. *Chem. Mater.* **2002**, *14*, 2078.
(42) Smith, D. E.; Dang, L. X. *J. Chem. Phys.* **1994**, *100*, 3757.
(43) Dauber-Osguthorpe, P.; Roberts, V. A.; Osguthorpe, D. J.; Wolff, J.; Genest, M.; Hagler, A. T. *PROTEINS: Structure, Function, and Genetics* **1988**, *4*, 31.
(44) Halgren, T. A. *J. Am. Chem. Soc.* **1992**, *14*, 7827.
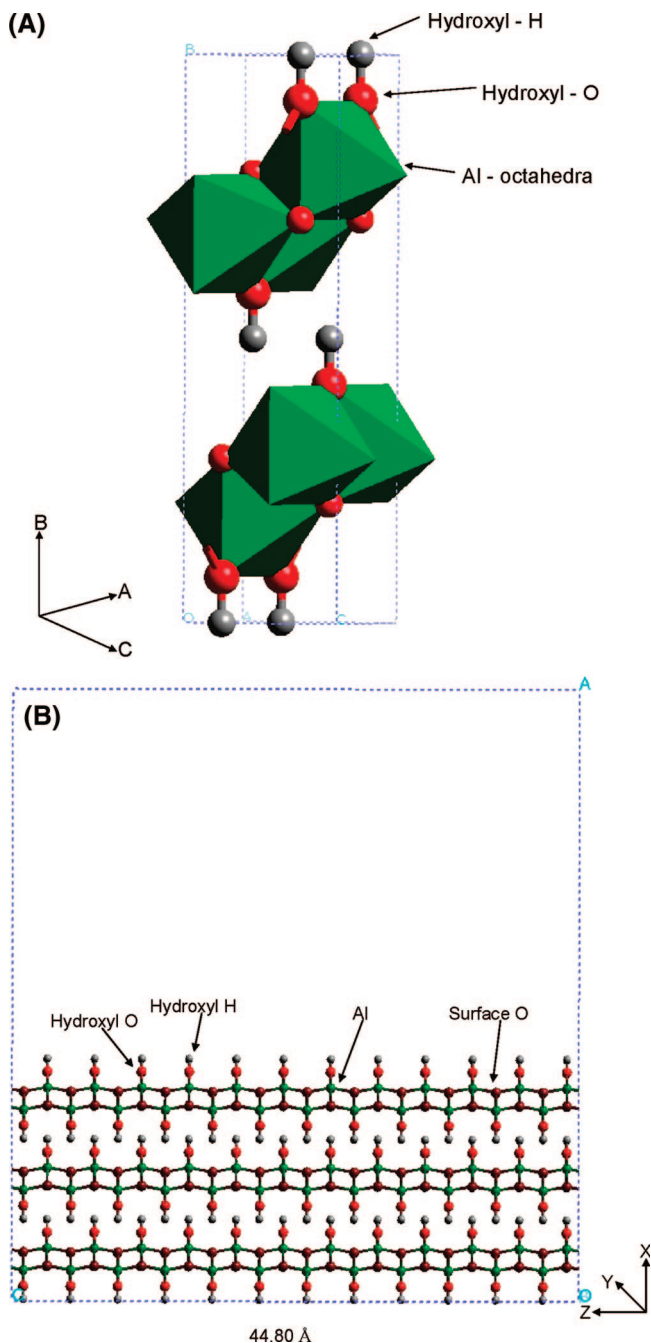(45) Accelrys, Inc., San Diego, CA.

(A)

Figure 1. (a) Polyhedron model of the γ-AlO(OH) unit cell. (b) γ-AlO(OH) (010) surface slab model used in molecular dynamics simulations.

cell structural data.[46] The boehmite unit cell (Figure 1a) was cleaved to create a completely hydroxylated basal (010) surface with no surface defects. The unit surface slab created was replicated to form a surface slab model with a depth of three layers (~18 Å) and a 37.3 Å × 44.3 Å (010) surface. A 30 Å vacuum gap was added to the system above the (010) surface to complete the slab model representation. The *x*-axis of the simulation cell is parallel to the crystallographic *b*-axis [010]; the *y*-axis is aligned with the *a*-axis [100]; and the *z*-axis is parallel to the *c*-axis [001]. Henceforth, we only reference the *xyz* coordinate system of the simulation cell. Atom types, charges, and masses were assigned to the atoms

(46) Hill, R. J. *Clays Clay Miner.* **1981**, *29*, 435.

in the simulation cell based on the CLAYFF force field. Maintaining an orthogonal simulation cell and fixing the vertical (*x*) direction, the total potential energy (Figure 1b) was minimized to optimize the atomic positions and cell dimensions associated with the "cleaved" (010) boehmite surface. The final dimensions of the minimized supercell used for the remainder of the simulations were 48.3 Å × 38.3 Å × 44.8 Å. Because the simulations are performed with cells having periodic boundary conditions, our models mimic idealized perfect surfaces free of defects, fractures, and grain boundaries. In addition, because of its periodicity, the system is effectively a series of thin boehmite slabs separated by 30 Å gaps in the [010] direction.

The gold (111) surface model was created in a similar manner from the crystallographic unit cell.[47] The unit cell was cleaved to create the (111) surface. The surface slab was replicated to form a large supercell. An orthogonal box was then cut from the nonorthogonal gold (111) supercell containing 1664 Au atoms. This surface slab model was energy minimized with atomic positions and the two lateral dimensions allowed to vary while maintaining an orthogonal simulation cell. The gold (111) simulation box (37.4 Å × 46.0 Å × 46.5 Å) was designed to be similar in size to that for boehmite in order to compare equivalent levels of hydration in subsequent simulations.

Hydration of Boehmite (010) and Gold (111). In the first molecular dynamics simulation involving surface hydration, the boehmite surface was initially equilibrated without water. The dynamics simulation was performed as a canonical ensemble (constant *NVT*; *N* = number of particles, *V* = volume, and *T* = temperature) at 298 K for 100 ps of simulation time using a 1 fs time step. We observed that both the energy and the temperature equilibrated for these systems within the first 10 ps. In subsequent simulations, incremental amounts of water were added to the surface of each system—from submonolayer coverage until the vacuum gap of the simulation cell was completely saturated with water molecules. For each increment in hydration, the system was equilibrated for 10 ps prior to collecting statistics for 20 ps using the NVT ensemble. The gold (111) simulations were performed using the same procedure as for boehmite (010).

Boehmite (010) Surface with Salt and Water. Na$^+$ and Cl$^-$ ions were added to the boehmite (010) simulation cell to examine the distribution of ions and evaluate the role of Cl$^-$ adsorption in pit corrosion. The Na$^+$ ions are included in the simulation cell to charge balance the Cl$^-$ ions. For the first simulation with NaCl solution, five Na$^+$ and five Cl$^-$ ions were added to a simulation cell that contained the boehmite surface slab pre-equilibrated with 3.5 monolayers of water. The aqueous concentration of NaCl is approximately 0.57 M. The ions were placed greater than 5 Å apart and vertically in the central region of the 3.5 monolayers of water associated with the boehmite surface (Figure 2a). In a second simulation, 15 Na$^+$ and 15 Cl$^-$ ions (0.48 M NaCl) were added to a simulation cell containing the boehmite (010)

(47) *Selected Powder Diffraction Data for Minerals*; Berry, L. G., Ed.; Joint Committee on Powder Diffraction Standards: Swarthmore, PA, 1974.
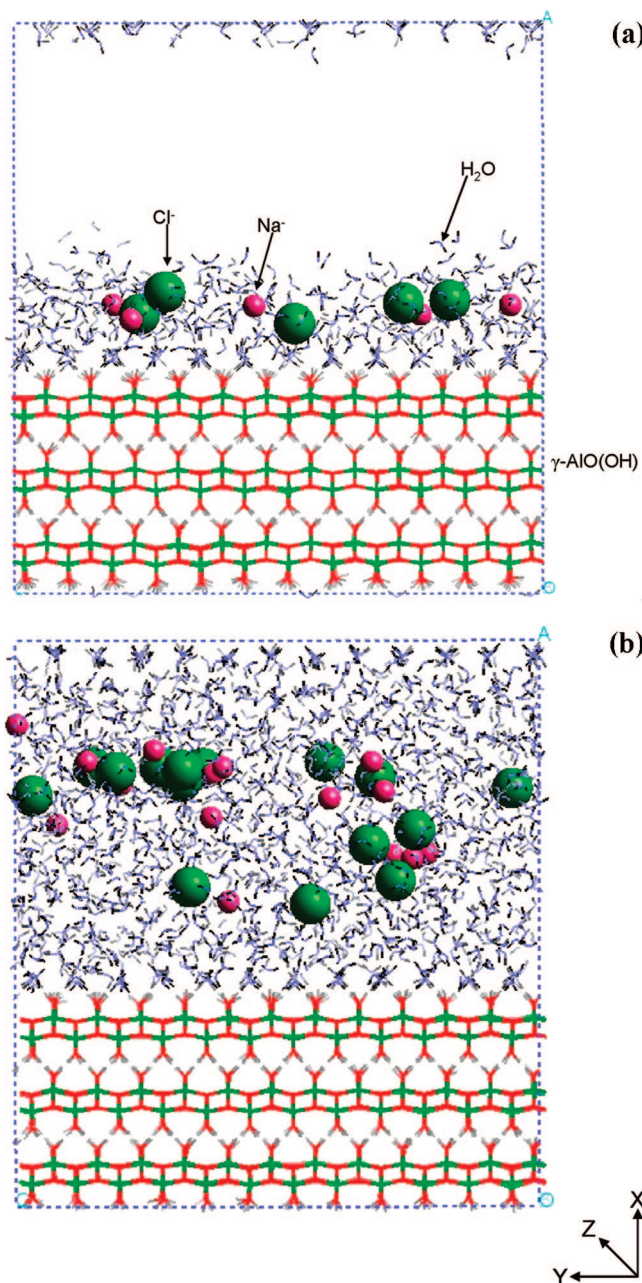
Figure 2. Simulation cells for boehmite–water–salt systems. (a) γ-AlO(OH) (010) surface with 2.5 monolayers of water with the addition of five Na$^+$ and five Cl$^-$ ions; ~0.7 M NaCl. (b) γ-AlO(OH) (010) surface with water-saturated volume and fifteen Na$^+$ and Cl$^-$ ions; ~0.5 M NaCl.

Figure 3. Average hydration energy as a function of the number of adsorbed water molecules on the γ-AlO(OH) (010) surface. Inset shows details of the changes in hydration layer as water molecules are added to the first monolayer. The surface coverages are noted for selected hydration states.

surface pre-equilibrated with bulk water (~10 monolayers). The ions were placed 15 Å above the boehmite surface and more then 5 Å apart (Figure 2b). MD simulations for both systems were performed under the same *NVT* conditions as previously for 500 ps. Atomic trajectories and energies were stored every 10 time steps (0.01 ps) for later analysis.

Results

Hydration Energy and Atomic Density Maps of the Boehmite Surface. The hydration energy for the boehmite–water interface as a function of adsorbed water is presented in Figure 3. The hydration energy provides information about the stability of the water molecules and their interactions with the boehmite surface. The inset in Figure 3 is an expanded version of the same plot for low surface coverages,
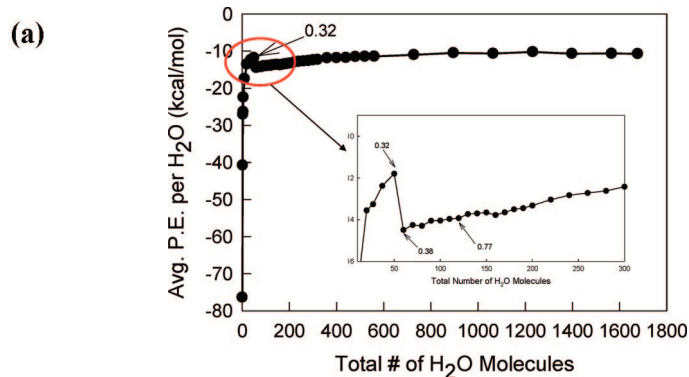
ranging from 0.04 (i.e., 6 H$_2$O molecules) to 1.8 monolayers (i.e., 280 water molecules). The surface coverage is calculated by determining the number of adsorbed water molecules relative to the number of surface sites or surface hydroxyl groups. The total number of water molecules that can coordinate to the boehmite surface in the simulation cell is 156. The simulations show evidence of a second monolayer of water starting to form before the first monolayer is complete; the boehmite surface is not completely covered by a single layer of water until the system is hydrated with water molecules to form over 1.5 monolayers.

The negative hydration energy $\Delta E_{\text{Hydration}}$ for a single adsorbed water molecule on the surface confirms the hydrophilic nature of the interactions on the boehmite surface. The hydration energy is defined as the difference in potential energy between a surface with *N* adsorbed water molecules $E(N)$ and the anhydrous surface $E(0)$ divided by the number (*N*) of water molecules:

$$\Delta E_{\text{Hydration}} = [E(N) - E(0)]/N \qquad (2)$$

The hydration energy increases as 50 water molecules are incrementally added to the boehmite surface.

Between surface coverages of 0.32 (i.e., 50 water molecules) and 0.38 (i.e., 60 water molecules), there is a favorable drop of over 2 kcal/mol in the hydration energy (Figure 3, inset). This decrease is associated with an increase in hydrogen bonding both between boehmite and water and among different water molecules (Figure 4a,b). Figure 4a shows a map of atomic density for the boehmite (010) surface at the 0.32 surface coverage. Area A illustrates a water molecule that is hydrogen-bonded to the surface. The gray contour denotes the surface hydroxyl hydrogen that is displaced by the water hydrogen atoms (black contour). Area B illustrates the reorientation of hydroxyl hydrogen atoms (gray contours) coordinated to the water oxygen atoms (blue contours). Area C shows hydrogen bonding between the water hydrogen atoms and the surface hydroxyl oxygen atoms. The total number of water hydrogen bonds between the boehmite surface and the water molecules was determined by counting displaced surface hydroxyl hydrogen atoms. The total number of hydrogen bonds among water molecules was determined by examining the orientation of the water hydrogen atoms (as in area D). There is an average of 56
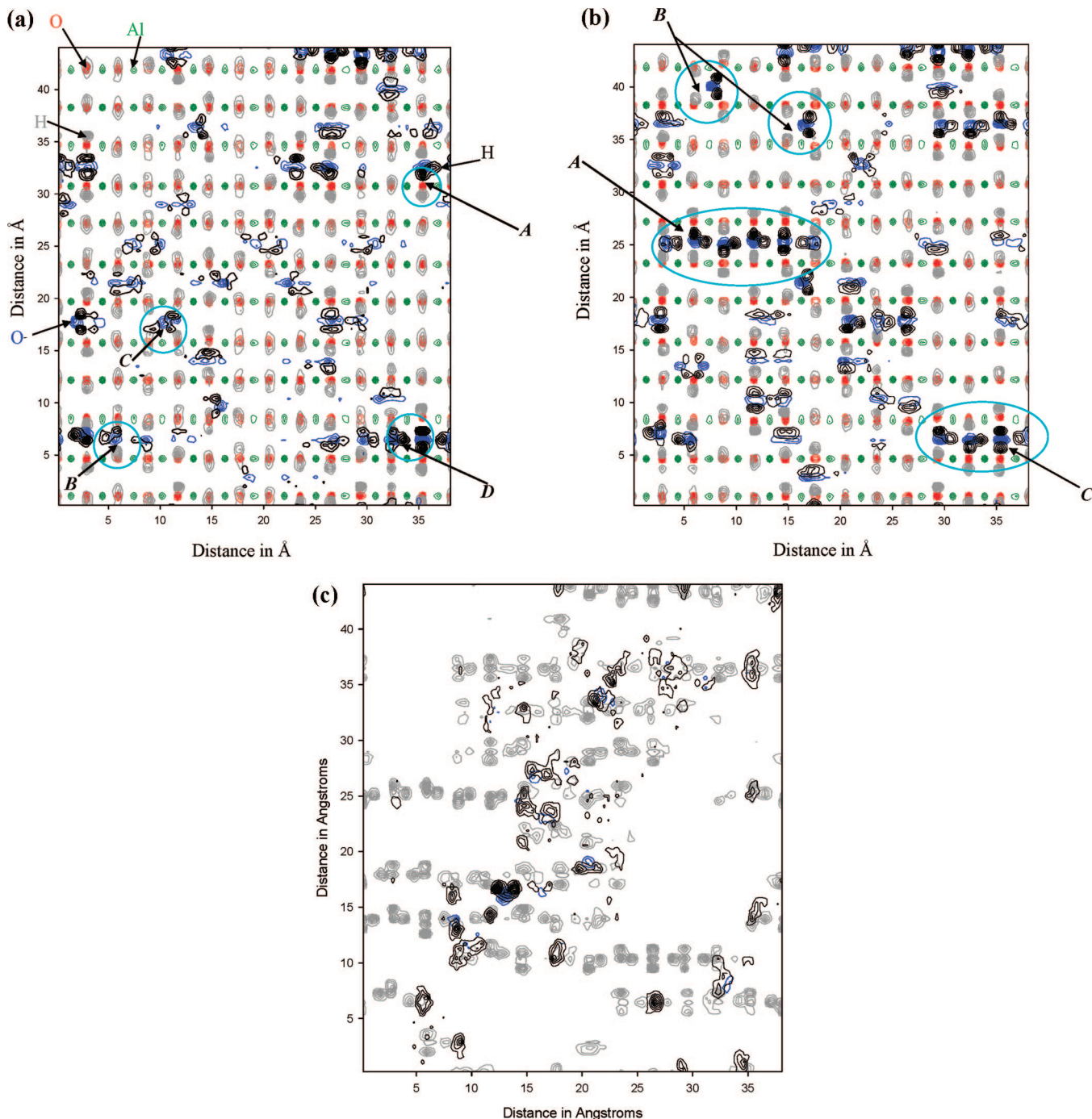
Figure 4. Atomic density maps for water on boehmite (010) surface viewed along the *x*-axis, normal to the surface. On (a) and (b), the green contours are Al, red contours are hydroxyl O, gray contours are hydroxyl H, blue contours are water O, and black contours are water H. (a) 0.32 surface coverage (50 H_2O molecules), (b) 0.38 surface coverage (60 H_2O molecules), and (c) 0.77 surface coverage (120 H_2O molecules) with a partial second monolayer. In (c) the gray contours are water molecules in the first layer of water, and the blue and black contours are water O and H in the second layer of water (>3 Å) above the surface. See text for discussion of circled areas.

boehmite−water hydrogen bonds and 15 water−water hydrogen bonds over the 20 ps simulation time for the 0.32 surface coverage. The ratio of the number of boehmite−water hydrogen bonds to the number of adsorbed water molecules is 1.12, and the ratio of water−water hydrogen bonds to the number of adsorbed water molecules is 0.30.

A change in hydrogen bonding is observed with the equilibration of an additional 10 water molecules. Figure 4b shows the contour map of the boehmite (010) surface at 0.38 surface coverage. There is an increase in the number of water molecules associated in a linear fashion, bonding to each other as shown in Area A, Figure 4b. There are four new groups comprised of three or more water molecules formed on the surface. Strongly adsorbed and isolated water molecules form four hydrogen bonds to the surface and prefer to adsorb between aluminol groups (Area B, Figure 4b). The water molecules that occur in linear chains occupy the sites between hydroxyl oxygen atoms (Area C, Figure 4b). The boehmite (010) surface exerts a crystallographic control on the water molecules (forming linear chains), and this organization of water allows additional hydrogen bonding among the molecules. This increase in hydrogen bonding

Water and Halide Adsorption to Corrosion Surfaces

Chem. Mater., Vol. 20, No. 14, 2008 4687

leads to a significant and stabilizing decrease in the hydration energy. The total number of boehmite−water hydrogen bonds is 74, and the number of water−water hydrogen bonds is 25. This provides an average of 1.23 boehmite−water hydrogen bonds per water molecule, and 0.41 water−water hydrogen bonds per water molecule in the system. The change in water−boehmite bonding and energetics between 0.32 and 0.38 coverage suggests that there is a threshold coverage associated with creating water-molecule chains on the boehmite surface. This threshold coverage will be a function of the random spatial distribution of water molecules on the surface and cannot be precisely characterized without detailed statistical analysis of many molecular simulations with different initial water arrangements.

As the number of water molecules added to the system increases beyond 280 (surface coverage of 1.8) there is a steady rise in the hydration energy (Figure 3). Additional water−water interactions occur through the formation of the second monolayer of water before the first monolayer has been completed. This process initially occurs (Figure 4c) at 0.77 surface coverage and continues until the exposed boehmite surface is fully covered with adsorbed water. The increase in hydration energy is attributed to increased interactions among water molecules rather than between the surface and the adsorbed water. As more water molecules are added to the system, the hydration energy approaches the limiting value of −9.95 kcal/mol which is equivalent to the calculated self-interaction energy for bulk water calculated using the flexible SPC water model. At a 0.77 surface coverage, 147 boehmite−water hydrogen bonds exist. The number of hydrogen bonds among water molecules is 78. The average number of boehmite−water hydrogen bonds per water molecule remains unchanged at 1.23 (the same as for the lower (0.30) surface coverage), but the average number of water−water hydrogen bonds per water molecule has increased to 0.65.

Atomic Density Profiles and Dipole Plots of the Boehmite (010) Surface. Atomic density profiles provide information about the orientation of water molecules near the surface, the local ordering of these molecules, and how additional monolayers of water affect surface–water interactions. These profiles are constructed by taking thin volume slices (typically 3 Å thick) of the simulation cell parallel to the surface. The number of each unique atom type in each volume is counted by analysis of the trajectory data to produce an atomic density for a given atom. For the boehmite (010) surface, atomic density profiles were derived parallel to the x-axis and normal to the boehmite surface (see Figure 1b).

Figure 5a is the density profile for the boehmite (010) surface at a 0.38 surface coverage (60 H_2O molecules). The first 19 Å of the profile represent the atomic positions associated with the boehmite (010) surface structure. The adsorbed water above the boehmite is indicated by two hydrogen peaks at 19.2 and 20.3 Å and an oxygen peak at 19.9 Å. Most water hydrogen atoms (57%) are positioned close to the boehmite surface and represent a tightly bound and structured water layer. The sharp H peak at 19.2 Å and O peak at 19.9 Å indicate that these water molecules are

very ordered with respect to the surface. The remainder of the hydrogen atoms, associated with similarly disposed oxygen atoms, is directed away from the surface and forms a more diffuse hydrogen profile while interfacing with the vacuum region above the interfacial region. Figure 5b illustrates the direction and magnitude of the x-component (vertical component normal to the boehmite surface) of the water dipole. The negative values near the surface of boehmite indicate that the water dipole points away from the surface. This is consistent with the highly structured orientation of water such that one H atom bonds to the O atom of the boehmite surface hydroxyl groups as indicated by the atomic density profile. The attraction of the water hydrogen atoms to the oxygen atoms at the boehmite surface is stronger than either hydrogen-bonding among water molecules or H−H repulsion between the hydrogen atoms of the water molecules and those of the surface hydroxyl groups.

As a monolayer of water forms on the boehmite surface, the orientation of the water molecules with respect to the surface remains constant. Water molecules contribute to the formation of a second monolayer before the first monolayer is completed. Figure 5c shows a density profile from a simulation with 728 water molecules or approximately 4.5 monolayers of water above the boehmite surface in the simulation cell. The first monolayer of water is indicated by a H peak at 19.4 Å and a sharp O peak at 20 Å. Again, the majority of the water molecules in the first monolayer of water have one hydroxyl group pointed toward the boehmite surface. A broad hydrogen peak between 21 Å and 22 Å represents the superpositioning of hydrogen atoms from water molecules in the first and second monolayers. The second broad and less intense O peak at 22 Å defines the location of the second layer of structured water that has developed. This peak and the H peak at 23.5 Å are broader than those observed closer to the boehmite surface because the water molecules are less organized and behave more like bulk water.

Figure 5d illustrates the interaction of bulk water with the boehmite surface. Once again the water molecules near the surface are organized with most of the hydrogen atoms interacting with the surface. The second O peak and next two H peaks continue to exhibit some structure as influenced by electrostatic interactions with the surface. Water above the first two monolayers is randomly oriented like bulk water. Figure 5e shows the magnitude and direction of the water dipole with respect to the boehmite surface as a function of distance away from that surface. The negative values near the boehmite surface denote a mean water orientation with the hydrogen atoms pointed toward the surface hydroxyl groups. At greater distances from the interface, the positive values suggest a mean water molecule orientation with the hydrogen atoms directed away from the surface. Values near zero indicate randomly oriented water molecules.

The accumulation of additional water molecules in the simulation cell has little effect on the orientation of the water molecules near the boehmite−water interface. Both the atomic density profiles and the sign of the vertical dipole component show that the water molecules in the first
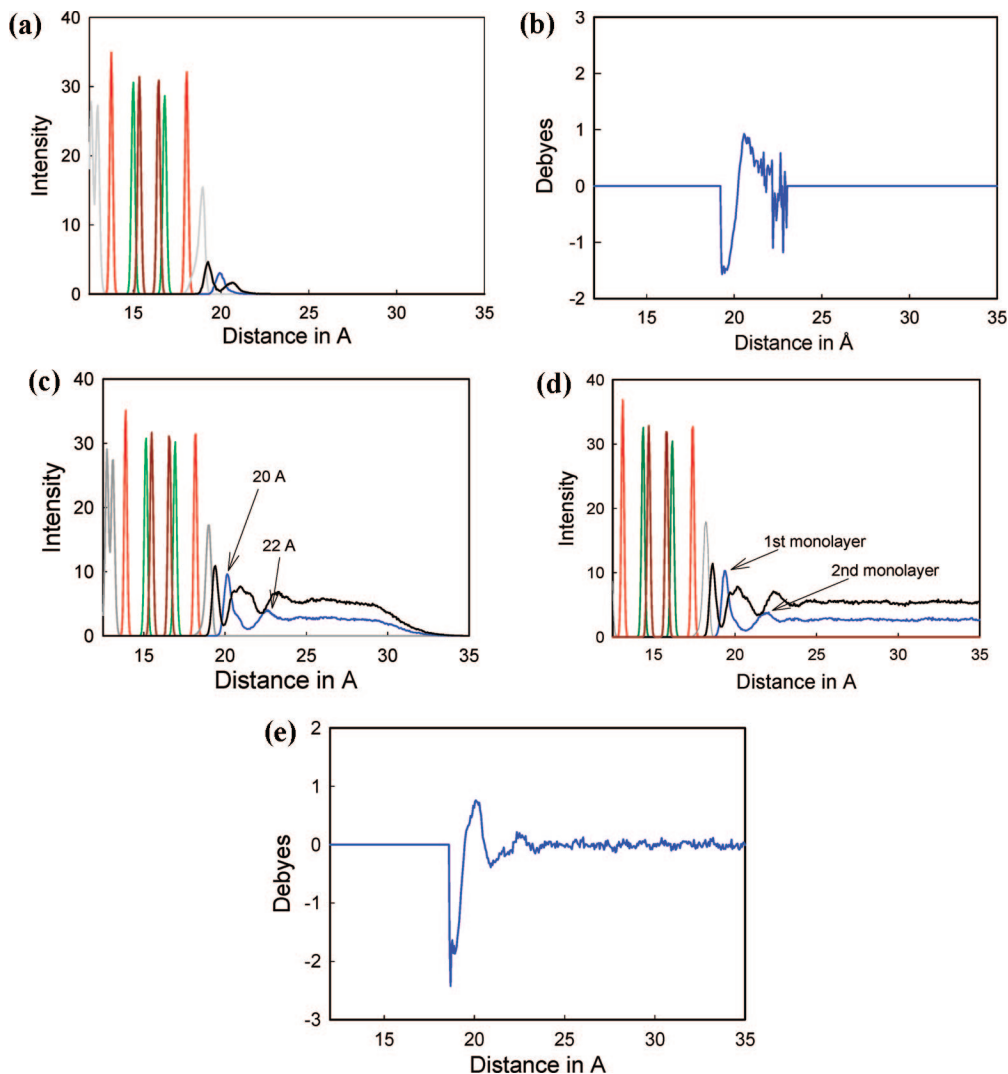
Figure 5. Atomic density and water dipole orientation profiles for the γ-AlO(OH) (010) surface. Green lines are Al, dark red lines are bridging O, red lines are hydroxyl O, gray lines are hydroxyl H, blue lines are water O, and black lines are water H. (a) Atomic density profile for 0.38 surface coverage (60 H_2O molecules), (b) dipole orientation profile for 0.38 surface coverage (60 H_2O molecules), (c) atomic density profile for 4.7 (728 H_2O molecules) monolayer coverage, (d) atomic density profile for water-saturated system, and (e) dipole orientation profile for water-saturated system.

adsorbed monolayer are oriented with at least one hydroxyl group pointing toward the surface. This interfacial structure is maintained as the system evolves to a fully hydrated interface.

Hydration Energy and Atomic Density Maps of Gold (111) Surface. Hydration energy and atomic density maps were also generated from the gold (111) surface MD trajectories. Figure 6 displays the average hydration energy on the gold (111) surface as a function of adsorbed water. The surface coverage was calculated in the same manner as previously for the boehmite (010) surface.

The hydration energy for the first adsorbed water molecule on the gold (111) surface is -7.0 kcal/mol. This suggests the gold surface is hydrophobic compared to the boehmite (010) surface where the hydration energy for one adsorbed water molecule is an order of magnitude more negative (approximately -70 kcal/mol). The addition of a second water molecule results in the formation of a water dimer on the gold (111) surface and lowers the hydration energy to -8.8 kcal/mol. The decrease in hydration energy between
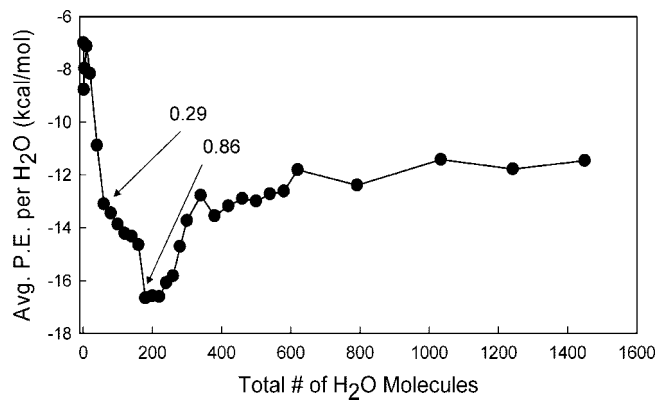

Figure 6. Average hydration energy as a function of the number of adsorbed water molecules on the Au(111) surface.

0.10 and 0.29 surface coverage is due to the formation of a hydrogen-bonded network among the water molecules. Figure 7a,b illustrates that the water molecules cluster together rather than associate freely with the gold (111) surface.
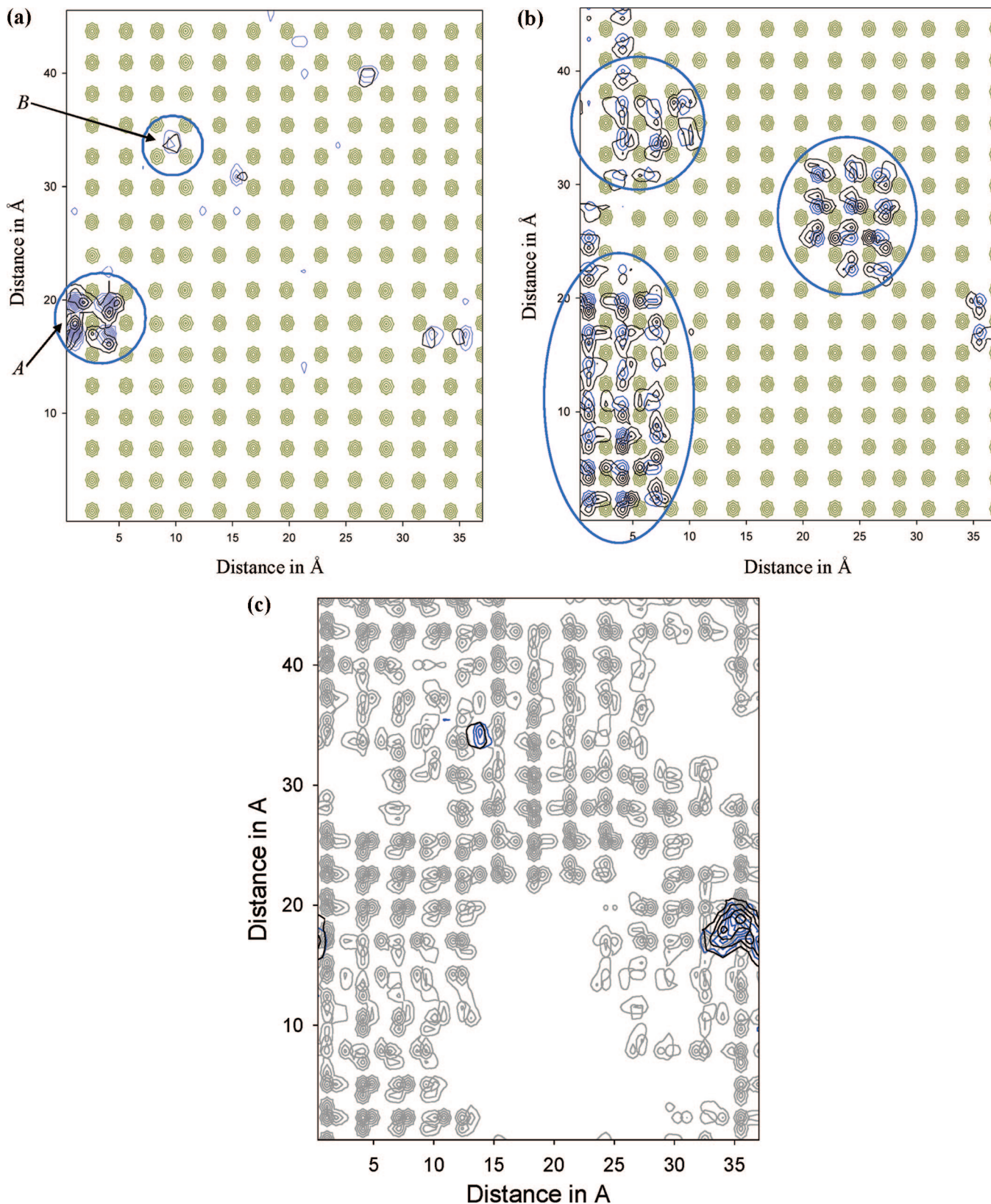
Water and Halide Adsorption to Corrosion Surfaces

Chem. Mater., Vol. 20, No. 14, 2008 4689

Figure 7. Atomic density maps for water on Au(111) surface viewed along the *z*-axis, normal to the surface. Yellow contours are Au, blue contours are water O, and black contours are water H. (a) 0.10 surface coverage (20 H_2O molecules), (b) 0.29 surface coverage (60 H_2O molecules), and (c) 0.86 surface coverage with a partial second monolayer of water. In (c), the gray contours are water molecules in the first layer of water, and the blue and black contours are water O and H in the second layer of water (>3 Å) above the surface. See text for discussion of circled areas.

Figure 7a illustrates the gold (111) surface with 0.10 coverage (20 H_2O molecules). Dense contour lines indicate relatively long residence times for atoms in given locations. Nine of the 20 molecules in the simulation cell adsorbed on the surface indicated in Figure 7a; the remaining 11 molecules adsorbed to the periodic image of the gold surface above the simulation cell. The black contour lines represent water hydrogen atoms, and the blue contour lines repre-
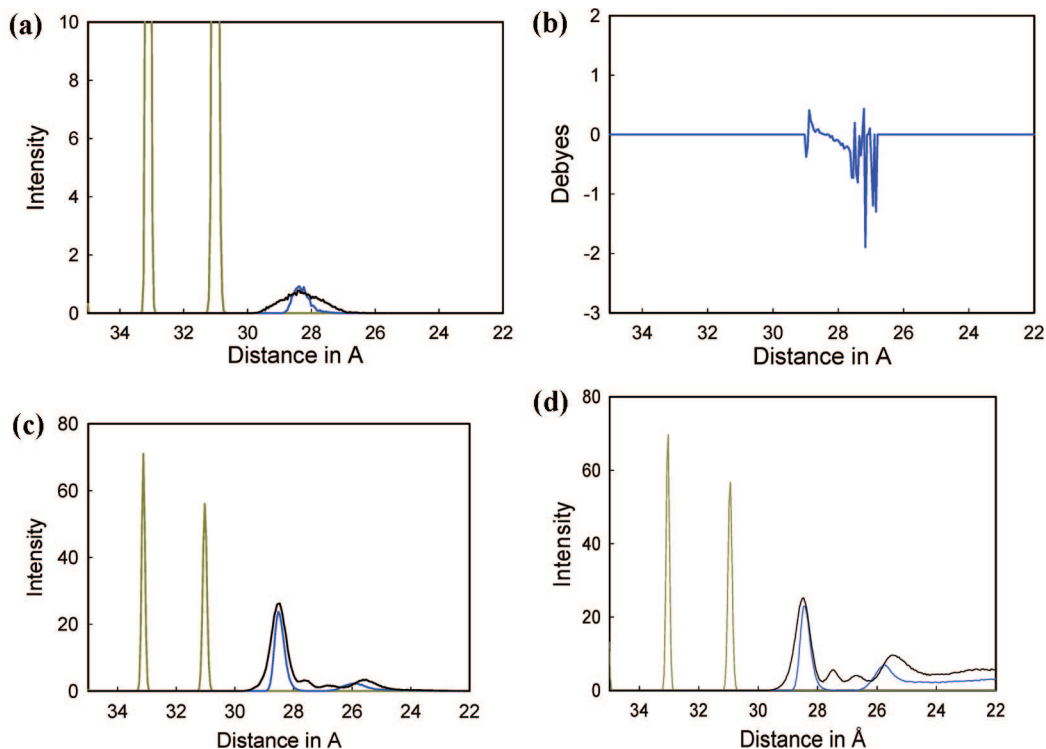
Figure 8. Atomic density and dipole orientation profiles of Au(111) surface. Yellow lines represent Au atoms, blue lines represent O atoms, and black lines represent H atoms. (a) Density profile 0.10 surface coverge (20 H_2O molecules), (b) dipole orientation profile for 0.29 surface coverage (60 H_2O molecules), (c) atomic density profile for 1.5 monolayer coverage (300 H_2O molecules), and (d) atomic density profile for 5 monolayer coverage (1034 H_2O molecules).

sent water oxygen atoms. In the area marked A there are four water molecules that form a hydrogen-bonded cluster. The other five molecules (example in area B) are isolated and dynamically interact with the gold surface during the MD simulation.

Figure 7b shows three distinct clusters (indicated by cyan circles) of water forming internally hydrogen-bonded networks on the gold. These networks help to stabilize the water molecules on the surface leading to a decrease in the hydration energy. This trend continues until 0.86 surface coverage (see Figure 6). The hydration energy increases toward the representative value for bulk water (−9.95 kcal/mol) as water molecules form a second monolayer before the first layer is completed (Figure 7c).

The minimal interaction between the water molecules and the gold (111) surface allows for the water molecules to form a hydrogen-bonded network among each other. The interaction between water and the gold (111) surface is controlled solely by van der Waals forces in our force field model. The simulations indicate the gold (111) surface does not exert crystallographic control on the water; instead the hydration energy is largely controlled by water−water interactions.

Atomic Density Profiles and Dipole Plots of Gold (111) Surface. As shown through the atomic density maps discussed above, adsorbed water behaves differently on the gold (111) surface than on the boehmite surface. This difference is also exhibited in the atomic density profiles and dipole orientation plots for the gold (111) surface. The gold (111) density profile is obtained parallel to the *z*-axis and normal to the gold (111) surface.

Figure 8a shows two overlapping peaks for O and H atoms of water at approximately 28.5 Å in the atomic density

profile. Both peaks are broad, and the water hydrogen atoms are evenly distributed on either side of the central O peak. The relatively broad density peaks indicate unstructured water with no preferred orientation with respect to the gold (111) surface. The dipole orientation data for a simulation (Figure 8b) confirm the diffuse nature of water molecules on the Au(111) surface. The water molecules, situated between 26 and 29 Å, freely reorient showing minor influence by the substrate.

As more water molecules are added, the behavior of the water at the gold surface changes. The initial diffuse layer at the surface becomes more ordered due to hydrogen bonding among the water molecules. For 1.5 monolayers of water, Figure 8c illustrates a sharp oxygen peak around 28.5 Å and a broader peak at 26 Å. The broader peak is associated with the diffuse second monolayer of waters forming on top of the more ordered first monolayer. The water hydrogen atoms are oriented in two different orientations, one group facing up into the vacuum space away from the gold (111) surface and the other group forming hydrogen bonds with the water layer below.

With half of the vacuum space of the simulation cell filled with water (1034 H_2O molecules) two sharp oxygen peaks are observed. In Figure 8d, two oxygen peaks are located at 28.5 Å and 26 Å. The first oxygen peak is associated with the ordered first monolayer of water discussed above. The second peak exhibits greater order than observed previously with the completion of successive monolayers of water. Beyond the second peak, the water is unstructured and exhibits the diffuse structure of bulk water.
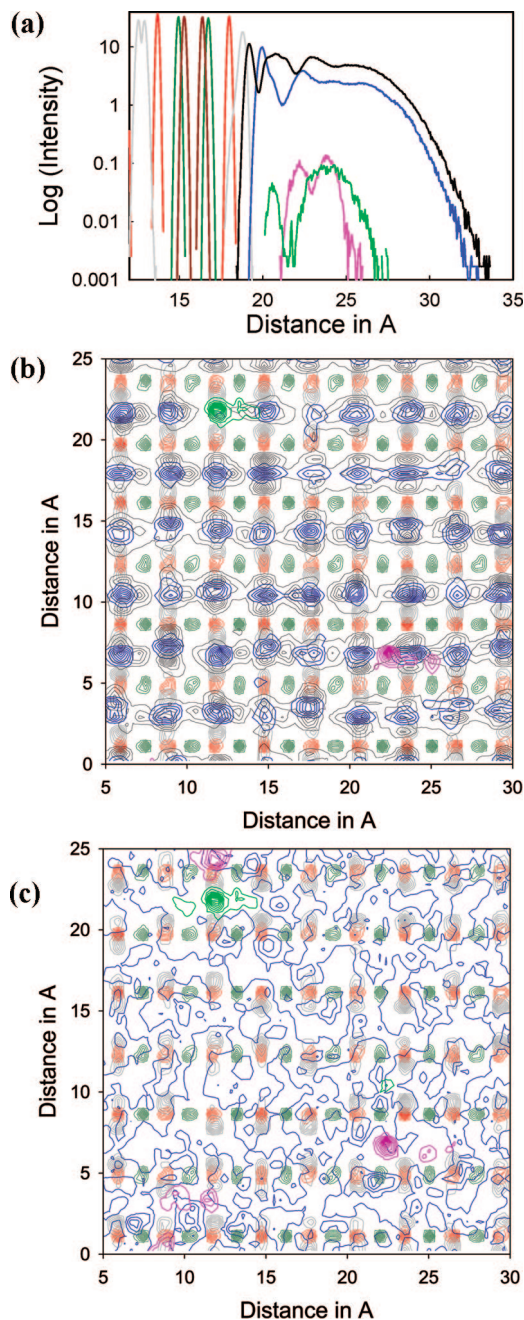
(a)

(b)

(c)

Figure 9. Atomic density profile and maps for 3.5 monolayers of water on γ-AlO(OH) surface with 5 Na$^+$ and 5 Cl$^-$ ions in solution. (a) Atomic density profile. Note that a log(intensity) scale is used to more clearly illustrate the relationship between structured water at the surface and the adsorbed Na$^+$ and Cl$^-$ ions. (b) Inner sphere (within 3 Å of surface) Na$^+$ and Cl$^-$. (c) Outer sphere (3−6 Å away from surface) Na$^+$ and Cl$^-$. Green represents Al, dark red represents bridging O, red represents hydroxyl O, gray represents hydroxyl H, blue represents water O, black represents water H, light green represents Cl$^-$ ions, and pink represents Na$^+$ ions.

Atomic Density of Boehmite (010) Surface with NaCl and Water. The initial simulation with NaCl was carried out with 3.5 monolayers of water and 5 Na$^+$ and 5 Cl$^-$ ions. Figure 9a presents the atomic density profile at the boehmite surface. The logarithm of the atomic density is used on the *y*-axis to compare the orientation of the water molecules with the position of the salt ions with respect to the surface. Chloride ions adsorb both as inner-sphere complexes, within the first monolayer of water, and are also located in the more diffuse second and third monolayers of water. Na$^+$ ions

adsorb to the surface at the same distance from the surface as the oxygen atoms of the second monolayer of water. A second peak in Na$^+$ concentration occurs in the third, more diffuse water layer.

Figure 9b presents an atomic density map for part of the boehmite surface that illustrates the adsorption on one Cl$^-$ and one Na$^+$ ion within 3 Å of the boehmite surface. The Cl$^-$ ion displaces the water molecules that were initially adsorbed to the surface. In contrast, the Na$^+$ ion does not disturb the prior arrangement of water molecules on the surface. Instead, Na$^+$ appears to sit between two water molecules in the first layer of water on the surface. Figure 9c illustrates the next 3 Å above the surface and the positions of Na$^+$ and Cl$^-$ ions that are adsorbed in the second layer of water as outer-sphere complexes within 3−6 Å of the boehmite surface. The orange circle (marked A) indicates the occurrence of an ion pair.

Results for the fully saturated boehmite simulation cell with 15 Na$^+$ and 15 Cl$^-$ ions again show that Cl$^-$ binds more closely to the boehmite surface than Na$^+$. Both ions are also present in more diffuse water away from the surface. Some of the Na$^+$ ions form small clusters on the surface, while others surficial Na$^+$ ions are paired with Cl$^-$ in the second monolayer of water. Small clusters of NaCl form on the boehmite surface in contact with bulk aqueous solution.

Discussion

Our examination of boehmite and gold surfaces by molecular dynamics simulations using an accurate force field provides an atomistic glimpse into the coordinated effort of water molecules to bind and cluster on surfaces as controlled by the relative strength of water−water and water−substrate interactions. Classical force field methods allow simulations of sufficiently large cells and substrate surface area to represent the water clusters and monolayers that form during atmospheric corrosion. Ab initio molecular dynamics and Car−Parrinello methods[21] may provide better accuracy and electronic structure details of surface hydration than classical force field methods but are impractical to examine the large-scale surface water structure presented in this study. To date, there are no molecular dynamics simulation studies of the hydration of boehmite or gold in the literature.

The boehmite (010) surface structure is similar to that of the (001) (Mg(OH)$_2$) brucite surface studied by Wang et al.[26,48] In addition, the simulated adsorption of water to boehmite (010) can readily be compared to that described by Wang et al.[26] for the (001) surfaces of brucite and gibbsite (Al(OH)$_3$). From Figure 4, it is evident that the surface hydroxyl (OH) groups of boehmite interact with each other forming vertical chains. Without the presence of water molecules, the boehmite surface hydroxyl hydrogen atoms (H$_{OH}$) oscillate between two positions above and below the hydroxyl oxygen atoms (O$_{OH}$), with maxima directly above the surface O$_{OH}$'s. The distance between neighboring surface O$_{OH}$'s in this direction is 3.7 Å, while the distance between them in the horizontal direction (as illustrated in Figure 4) is 2.9 Å. The hydroxyl groups are aligned because the H$_{OH}$'s

(48) Wang, J.; Kalinichev, A. G.; Kirkpatrick, R. J. *Geochim. Cosmochim. Acta* **2004**, *68*, 3351.

are each repelled by two neighboring Al atoms (1.9 Å) and attracted to four equidistant (2.8 Å) bridging oxygen atoms in the gibbsite structure.

The pattern created by the surface hydroxyl groups differs from those formed on the brucite and gibbsite surfaces. For brucite, the OH groups tilt with equal probability toward three neighboring tetrahedral vacancies on the surface, displaying a triangular distribution.[26] For gibbsite, there are two distinct populations of OH groups: one-third of them tilt slightly toward octahedral vacancies, while the other two-thirds are dynamically distributed between two preferred orientations.[26]

Chains of water molecules form on the boehmite surface (see Figure 4b) perpendicular to the chains of OH groups, with one water hydrogen atom above each bridging O atom of the boehmite surface structure. The water molecules form hydrogen bonds with each other and the surface hydroxyl groups. In addition, one of the two hydrogen atoms in each adsorbed water molecule is within a 4 Å distance from a bridging O atom. A single chain of water molecules on the surface imposes additional constraints on the motion of the OH groups. The hydroxyl groups in one chain all orient in the same direction (e.g., up) forming a series of hydrogen bonds. The OH groups in the neighboring chains orient in the opposite direction. A hydrogen-bonded network is thus formed between the water molecules and the surface hydroxyl groups.

Figure 5a,c,d provides the atomic density profiles for boehmite, with different water concentrations. To compare the position of the water molecules above the boehmite surface with those calculated for brucite and gibbsite, we measured the distance between the average position of the O_{OH}'s and the O_{H2O}'s. For the fully saturated system, the first O_{H2O} density maximum is 1.88 Å away from the surface oxygen atoms, and the second density maximum is 4.64 Å away from them. These two O_{H2O} density maxima are closer to the boehmite surface than those reported for brucite (2.40 Å and 4.95 Å) and gibbsite (2.55 Å and 5.10 Å).[26] The relative peak distances can be compared accurately because the simulations were all performed using the same force field.[36] Measurements of the positions of the two O_{H2O} peaks with respect to the surface were also compared for four different water concentrations. Although minor variations were observed (1.88−1.98 Å and 4.35−4.64 Å for the first and second maxima, respectively), a more detailed study would be necessary to determine if these variations are indicative of a trend.

The small bond distances formed between boehmite and surface water are probably a result of attraction between the H_{H2O}'s and the surface bridging O atoms that occur lower in the surface structure rather than the Al atoms. The basal surface of boehmite is hydrophilic. The hydroxyl-terminated surface sites provide both hydrogen bond donors and acceptors that interact with the first monolayer of water molecules, and the bridging oxygen atoms provide additional hydrogen-bond acceptors. We observed that the majority of water molecules in the first water layer are oriented with hydrogen toward the surface forming a hydrogen-bond network with the hydroxyl oxygen atoms of the boehmite.

Isolated water molecules exhibit more than two hydrogen bonds to surface hydroxyl groups. Above 0.30 surface coverage, a second layer of less tightly bound water with hydrogen atoms directed away from the surface starts to form. For the simulations involving multiple monolayers or bulk water, the water oxygen profile loses structure beyond 10 Å and becomes more diffuse.

It should be noted that although water molecules on the Au(111) surface orient freely on the surface and are not controlled by the crystal structure, water still forms at least two clearly distinct water layers at the gold surface. The first monolayer of water molecules is flat, parallel to the surface of Au atoms, with the water molecules forming a hydrogen-bonded network with each other. The second layer of water then forms hydrogen bonds with the first layer. From the atomic density profile illustrated in Figure 8d, it is evident that interfacial water at the gold surface also exhibits two to three relatively structured layers of water before losing structure beyond 7 Å from the surface.

Although no experimental measurements or molecular simulations of Na^+Cl^- adsorption or other electrolyte adsorption have been performed for boehmite prior to this study, molecular simulations have been performed to investigate cation and anion adsorption to other oxide surfaces. In one study, the Cl^- density profile for the neutral hydroxylated rutile (110) surface exhibited a small Cl^- peak resulting from the direct interaction with hydrogen atoms of the surface hydroxyl groups.[49] We also observed the adsorption of Cl^- ions on boehmite as an inner-sphere complex, directly interacting with the surface hydroxyl groups. Experimental measurements or other molecular simulations of electrolyte adsorption on boehmite are not available in the literature. We must rely on the quality of the force field parameters and previous parameter validation to judge the quality of the adsorption results for these ions.

Conclusions

By using an accurate energy force field and a series of molecular dynamics simulations, the hydration of boehmite (010) and gold (111) surfaces was successfully calculated. In addition, a set of simulations involving a NaCl electrolyte solution provided insight into the adsorption of Na^+ and Cl^- to the boehmite surface.

Water molecules strongly adsorbed to the boehmite (010) surface. The density profiles, atomic density, and dipole profiles indicate that water molecules in the first monolayer have a preferred orientation. The majority of these molecules form a hydrogen bond between a water hydrogen and surface hydroxyl oxygen. The attraction of water hydrogen to the surface hydroxyl oxygen is greater than the repulsion of the surface hydrogen to water hydrogen. As the water in the system approaches bulk behavior, the first monolayer remains intact with the majority of the water hydrogens bonded to the surface. The water molecules on the boehmite (010)

(49) Zhang, Z.; Fenter, P.; Cheng, L.; Sturchio, N. C.; Bedzyk, M. J.; Predota, M.; Bandura, A.; Kubicki, J. D.; Lvov, S. N.; Cummings, P. T.; Chialvo, A. A.; Ridley, M. K.; Bénézeth, P.; Anovitz, L.; Palmer, D. A.; Machesky, M. L.; Wesolowski, D. J. *Langmuir* **2004**, *20*, 4954.

surface occupy different sites depending on the extents of water coverage. Isolated water molecules on the surface prefer to occupy the sites between two surface aluminol groups. As more water is added to the simulation cell the water molecules prefer to occupy the sites between two surface hydroxyl oxygen atoms.

The water behavior at the gold (111) interface is significantly different relative to boehmite hydration. The first monolayer forms a hydrogen bonded network of water molecules rather than associating with the gold surface. There is minimal surface–water interaction. The atomic density plots and the density profiles exhibit an even distribution in the orientation of the water hydrogens. Nonetheless, for both boehmite and gold, the effect of the surface in structuring water is minimal after the second water layer.

The addition of NaCl electrolyte solution to the boehmite (010) simulation cell disrupts the first monolayer of water. The Cl^- ions in the 0.04 monolayer coverage simulation displace several waters in the first monolayer. The Na^+ ions that diffuse into the first monolayer do not displace any adsorbed surface waters. The Cl^- ions prefer sites between surface oxygen atoms, and the Na^+ ions prefer sites between surface aluminum atoms. Na^+-Cl^- pairs were observed to occur on the surface. Both the near-surface water structure and the effects of ion adsorption were similar regardless of the number of monolayers of water overlying the boehmite surface.

CM702781R